

RESEARCH PAPER

Super-wideband and compact omnidirectional antenna with simple structure and improved radiation properties

X. CHEN^{1,2}, L. YANG¹, L. WANG¹ AND G. FU^{1,2}

A super-wideband (SWB) omnidirectional antenna is reported in Lau et al. in 2005 and 2008, but the antenna structure was complex and the radiation properties were unsatisfactory. In this paper, a SWB omnidirectional antenna with simple structure and improved radiation properties is presented. The antenna just consists of a two-stage inverted cone and two shorting pins. The proposed two-stage cone can improve the impedance matching in super-wide bandwidth, and the optimized shorting pins can reduce the cut-off frequency more than 50%. The calculated and measured results are investigated to confirm the antenna performances. The impedance bandwidth of the antenna for voltage standing wave ratio ≤ 2 achieves more than 1:22.1, covering 0.905 GHz to the above band. The smaller sizes than those referred by Lau et al. in 2008 are obtained. The profile of the antenna is $0.078\lambda_c$ and the diameter of the radiation body is $0.217\lambda_c$ (λ_c is the wavelength of the cut-off frequency of the antenna). In addition, the radiation properties of the kind of SWB omnidirectional antenna are improved obviously. In the whole band, the ripple levels in horizontal radiation patterns are not more than 6.6 dB, and the cross-polarized levels are reduced by 9 dB.

Keywords: Omnidirectional antenna, Wideband, Miniaturization, Out of roundness, Cross polarization

Received 16 September 2015; Revised 26 March 2016; Accepted 4 April 2016

I. INTRODUCTION

The omnidirectional antennas are always the research hotspot due to their widely applications [1, 2]. As the requirement of multi-band and compact communication devices, the wideband and miniaturized omnidirectional antennas are demanded urgently [3, 4], e.g. the antennas for the indoor base stations and on-board mobile station. Monopole is the traditional omnidirectional antenna, and it is characterized by the nearly quarter-wavelength height and narrow-band operation, which cannot satisfy the current development.

Monopolar patch antennas are the low-profile omnidirectional antennas. In 1993, Delaveaud *et al.* first propose monopolar patch antenna which has a very low profile of 0.058λ and the like-monopole radiation pattern (RP) [5]. A patch is added on a low monopole and shorted to the ground. Its impedance bandwidth for voltage standing wave ratio (VSWR) ≤ 2 is merely 3%. After that, many monopolar patch antennas are investigated to reduce the sizes and enhance the bandwidth further [6–11]. Among them, some antennas achieve the

ultra-wideband (UWB) property. Lau *et al.* propose a kind of monopolar patch antenna whose impedance bandwidth reaches 138% (1:7.4) [1]. He adopts four orthogonally combining truncated trapezoidal plates as the feeding structure under the patch and grounds the patch with four symmetric thin wires. The profile and diameter of the monopolar patch are $0.087\lambda_c$ and $0.246\lambda_c$ separately, where λ_c is the wavelength of low cut-off frequency for VSWR ≤ 2 . Later, Lau improves the feeding structure further, and a super impedance bandwidth of more than 1:26 is obtained [2]. However, the antenna structure is very complex, and the roundness of the horizontal RP and the cross-polarization are both deteriorative. Recently Koohestani *et al.* put forward another UWB omnidirectional antenna, which almost has the same height with the Lau's antenna. A simply inverted cone is adopted as the feeding structure under the shorted patch, and the electromagnetic (EM) coupling is utilized to feed the patch. The space between the cone and the patch is also hardly to maintain [12].

It is an interesting problem that how to use the simplest structure to reach the best antenna performances. In this paper, we propose a simple omnidirectional antenna which also has the super-wideband (SWB) property, and the sizes of the antenna are smaller than those of the former SWB antenna [2]. In addition, the roundness of the horizontal RPs and the cross-polarization are both improved. Although the cone structures have been used in monopolar patch antenna, they are not about two-stage cone and the SWB

¹Science and Technology on Antenna and Microwave Laboratory, Xidian University, Xi'an Shannxi 710071, China. Phone: +86 13572915354

²Collaborative Innovation Centre of Information Sensing and Understanding, Xidian University, Xi'an Shannxi 710071, China

Corresponding author:

X. Chen

Email: xchen@mail.xidian.edu.cn

property has not been obtained. In Section II, the antenna configuration is presented. Then, the effect of the main structure parameters are analyzed in Section III. In Section IV, the experimental results are discussed. Finally, the conclusions are drawn.

II. ANTENNA CONFIGURATIONS

Figure 1 shows the configurations of the proposed antenna, which follows the principle of simplicity and practicability. It just consists of three components: a two-stage inverted cone, two shorting pins and a circular ground plane. All of the components are metal materials and connected directly. There are no unstable structures on that. The two-stage inverted cone is located at the center of the ground plane, and it can be seen as a union of a feeding cone (lower) and a radiation cone (upper). The structure of two-stage cone introduces new parameters, which can be adjusted for a

better antenna performance. In practice, when the feeding cone has a smaller cone angle than that of the radiation cone, a better impedance matching and a larger bandwidth will be obtained. In addition, if the height of the entire antenna is fixed, the proportion of radiation cone and feeding cone will be a crucial parameter, which affects the impedance matching clearly in the low band. These will be discussed in the next section. The two-stage cone is integrated together and do not need to be assembled, so it is more facilitated than others [2, 10, 12]. If a light weight is required further, the cone can be manufactured into a hollow body, or the cone could be manufactured by the plastic and electroplated on the surface. The bottom of the two-stage cone connects with the inner core of the radiofrequency (RF) connector, and the circular ground plane connects with the outer shield of the RF connector. The two shorting pins are another important component. They are two thick poles and symmetrically located at two-side edges of the two-stage cone. Their effects include connecting the radiation cone to the ground plane and supporting the cone structure. In [2], four thin wires of 1 mm diameter are used as the grounding structure for a better performance, but they are too thin to support the radiation body. Therefore, the extra supporting structure has to be settled. In our prototype, we just use two nylon poles at the orthogonal position of the shorting pins to keep the balance of the cone (Fig. 1(c)).

For a SWB antenna, its electrical sizes depend on the physical sizes of the antenna and the low cut-off frequency of VSWR. In our design, we determine the external dimensions of the antenna firstly and try to get the lowest cut-off frequency through the optimization of the parameters. Shown in Fig. 1, the maximum diameter of the two-stage cone $2R_p$ is fixed as 72 mm, and the height of the cone h_p is fixed as 26 mm. The diameter of the ground plane D_g is 296 mm, and its thickness is 2 mm. In the following section, the effect of the main parameters on the low cut-off frequency and the impedance bandwidth are analyzed. The EM simulation software CST MWS, based on Finite Integration Time Domain technology, is utilized to evaluate the performances of the wideband antenna.

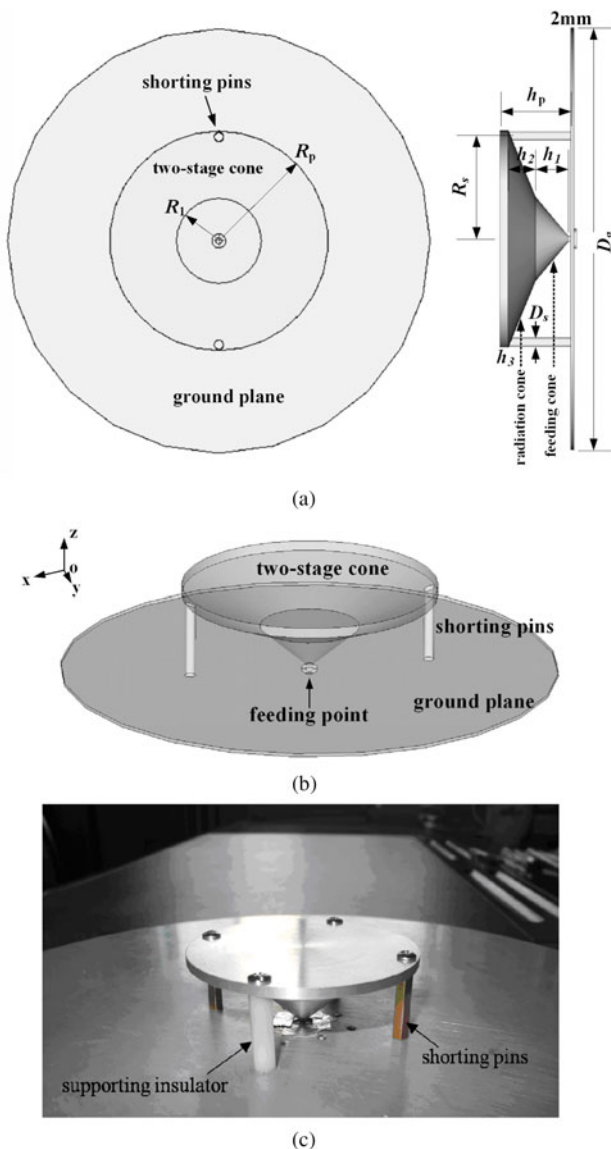


Fig. 1. Configurations of the proposed antenna. (a) Local view. (b) Full view. (c) Prototype of the antenna.

III. LOW CUT-OFF FREQUENCY AND SWB PROPERTY OF THE ANTENNA

The internal parameters of the antenna mainly include those of the shorting pins and the two-stage cone. The parameter studies are carried out to investigate the antenna structure. The given sizes include: $h_1 = 12$ mm, $h_2 = 10$ mm, $h_3 = 3$ mm, $R_1 = 14$ mm, $R_s = 32.4$ mm, and $D_s = 3$ mm.

A) Effect of shorting pins

The cases with and without shorting pins are calculated. Figure 2 gives the VSWR curves of the two cases. The calculating frequency range is set from 0.1 to 10 GHz to identify the variation clearly in the low band. The range will be set as 0.1–20 GHz later. From Fig. 2, both cases show the high-pass characters, but the low cut-off frequency of the case with shorting pins is much lower than that without shorting pins. The former is 0.9 GHz, while the latter is merely

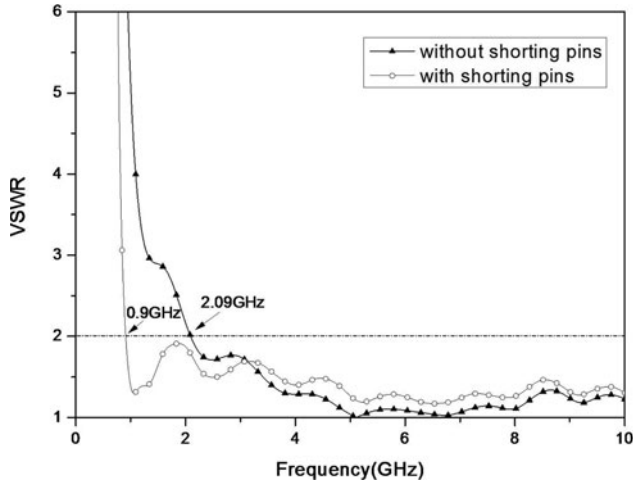


Fig. 2. VSWR of the proposed antenna with and without shorting pins.

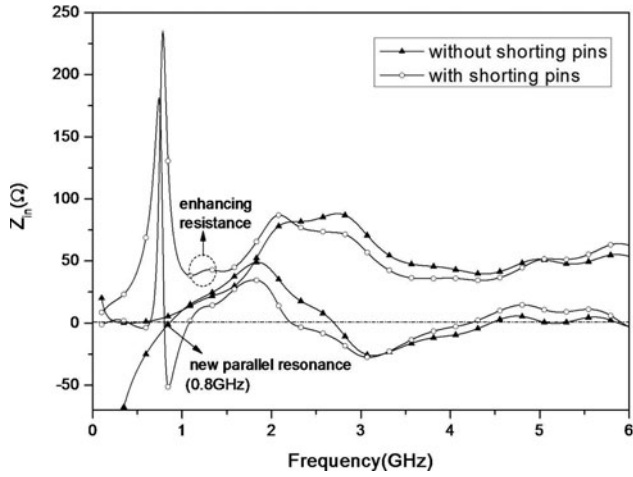


Fig. 3. Input impedance of the proposed antenna with and without shorting pins.

2.09 GHz. The low cut-off frequency is reduced by 57%. It is implied the dimensions of the antenna can be reduced more than a half by the shorting pins.

Figure 3 shows the input impedance curves of the two cases. Above 2 GHz, the curves of the two cases are almost same. While below 2 GHz, a new parallel resonance is aroused around 0.8 GHz after the shorting pins added. This parallel resonance enhances the values of the input resistance about 1 GHz, so the impedance matching of the cone can be solved from 0.9 to 2 GHz.

B) Diameter and position of shorting pins

The parameters of the shorting pins are the diameter and the position of the pins. The VSWR curves with different diameters are shown in Fig. 4. The diameter varies from 1 to 7 mm. In a global view, the VSWR curves change a little. The main changes occur in the low band (about 1~2 GHz). After enlarging the local view of the low band, the variation of the low cut-off frequency can be clearly observed. The lowest cut-off frequency is 0.9 GHz at $D_s = 3$ mm. When

$D_s = 1$ and 5 mm, the low cut-off frequencies are approximately equal. The frequency moves to 1.03 GHz when $D_s = 7$ mm. If the shorting pins are too thin, then the extra supporting structure has to be added [2].

The position of the shorting pins is expressed by a normalized parameter k_{short} which equals the ratio of R_s to R_p . Figure 5 shows the VSWR curves with different k_{short} from 0.7 to 1. As k_{short} decreases, the values of VSWR in low band increase quickly and the low cut-off frequency shifts to the lower frequency slightly. When $k_{short} = 0.9$, the low cut-off frequency and the impedance matching can achieve a good balance.

Therefore, the parameters of the shorting pins mainly affect the low cut-off frequency and the impedance matching in the low band.

C) Sizes of cone – h_1 and R_1

The crucial parameters of the two-stage cone are the internal ones h_1 and R_1 , which will decide the proportion of the two stage and the cone angles. Figure 6 shows the VSWR curves

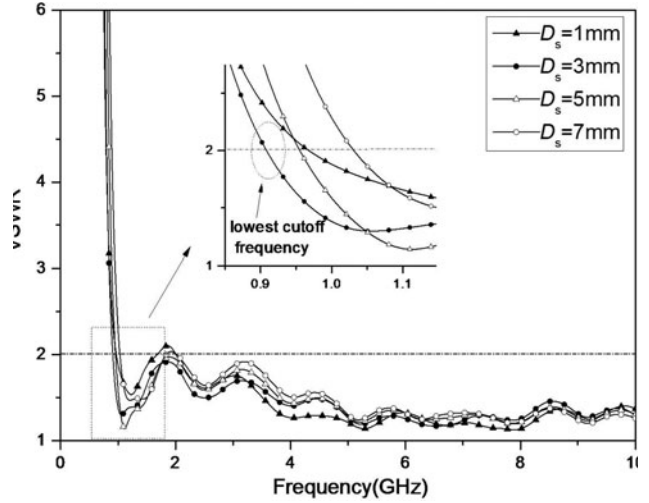


Fig. 4. VSWR with different diameters of shorting pins.

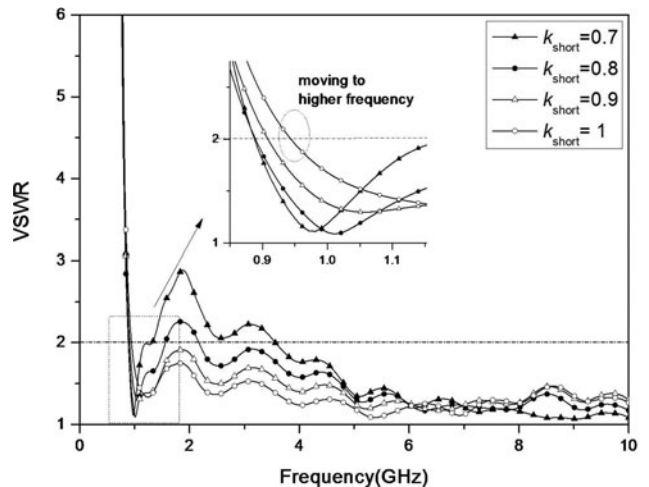
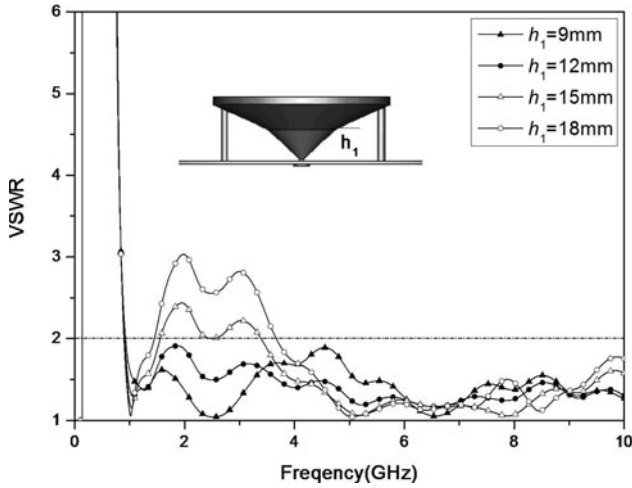


Fig. 5. VSWR with different positions of shorting pin.

Fig. 6. VSWR with different h_1 .

with different h_1 . As h_1 rises, the impedance matching deteriorates quickly in 1.5–3.5 GHz. When $h_1 = 9$ and 12 mm, the VSWRs are both well. However, the low cut-off frequency tends toward higher and the impedance matching tends to deteriorate at 4.5 GHz when $h_1 = 9$ mm.

The VSWR curves with different R_1 are shown in Fig. 7. When $R_1 = 8$ mm, the VSWR values are beyond 2 in 1.5–3.5 GHz and 6~7 GHz. As the radius increases, the impedance matching tends to balance in the whole band. When $R_1 = 20$ and 26 mm, the VSWR values are beyond 2 about 4 GHz, and the low cut-off frequencies also tend toward high frequency. When $R_1 = 14$ mm, the VSWR curve reaches a balance in the whole band.

In summary, h_1 and R_1 have little effect on the low cut-off frequency but mainly decide the impedance matching of the whole band, so they can be optimized further for the best impedance matching and bandwidth.

IV. EXPERIMENTAL RESULTS AND DISCUSSIONS

A prototype of the proposed antenna was fabricated to confirm the performances. Figure 1(c) shows the photograph of the antenna. The two-stage cone has an integrated structure. The measurement is carried out at microwave anechoic chamber at Xidian University. The frequency range of 0.1–20 GHz is observed. Figure 8 shows the measured VSWR comparing with the calculated one. The SWB property can be observed. The measured curve has the similar shape with the calculated one, but the measured values are higher than the calculated ones in medium and high band. It is due to the fabricating errors increasing as the frequency rises. The low cut-off frequencies of the two curves agree much well. The measured low cut-off frequency for $VSWR \leq 2$ is 0.905 GHz, while the calculated value is 0.9 GHz. Based on 0.905 GHz, the impedance bandwidth of the proposed antenna for $VSWR \geq 2$ is more than 1:22.1. The external electrical sizes of the antenna are $h_p = 0.078\lambda_c$ (26 mm) and $2R_p = 0.217\lambda_c$ (72 mm). The diameter of the ground plane is $0.893\lambda_c$ (296 mm). All of the three electrical sizes are smaller than those of the SWB monopolar patch antenna in reference [2].

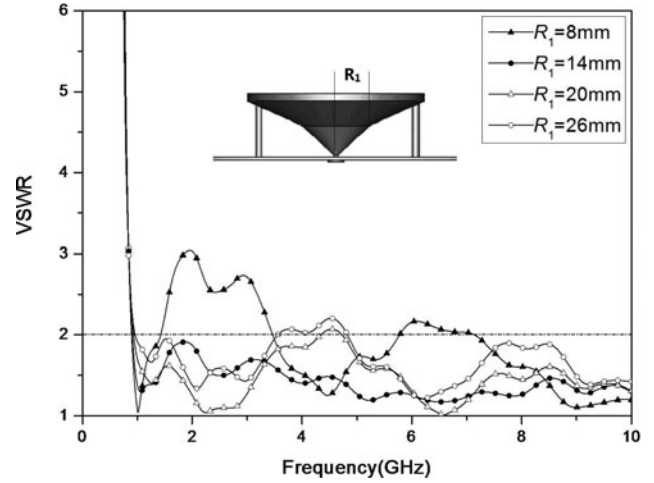
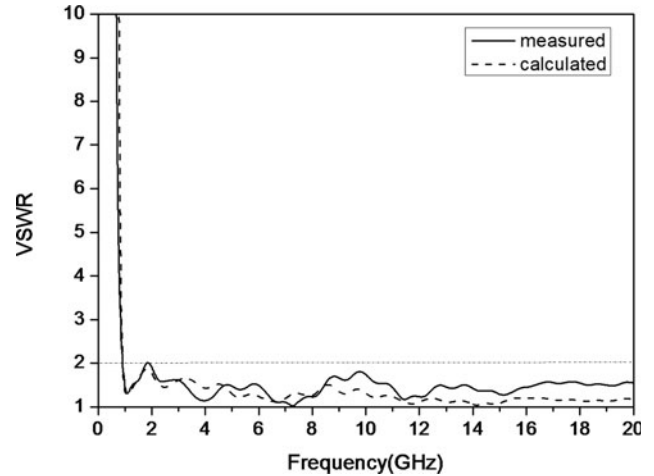
Fig. 7. VSWR with different R_1 .

Fig. 8. Measured and simulated VSWR of proposed antenna.

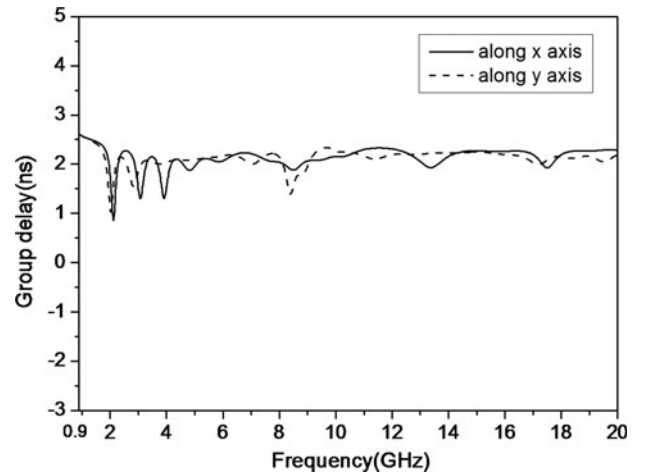


Fig. 9. Group delay of the proposed antenna system.

Such a super bandwidth almost covers the band above 1 GHz, and multi-band operations can adopt the proposed antenna. When the antenna is used in UWB systems, the

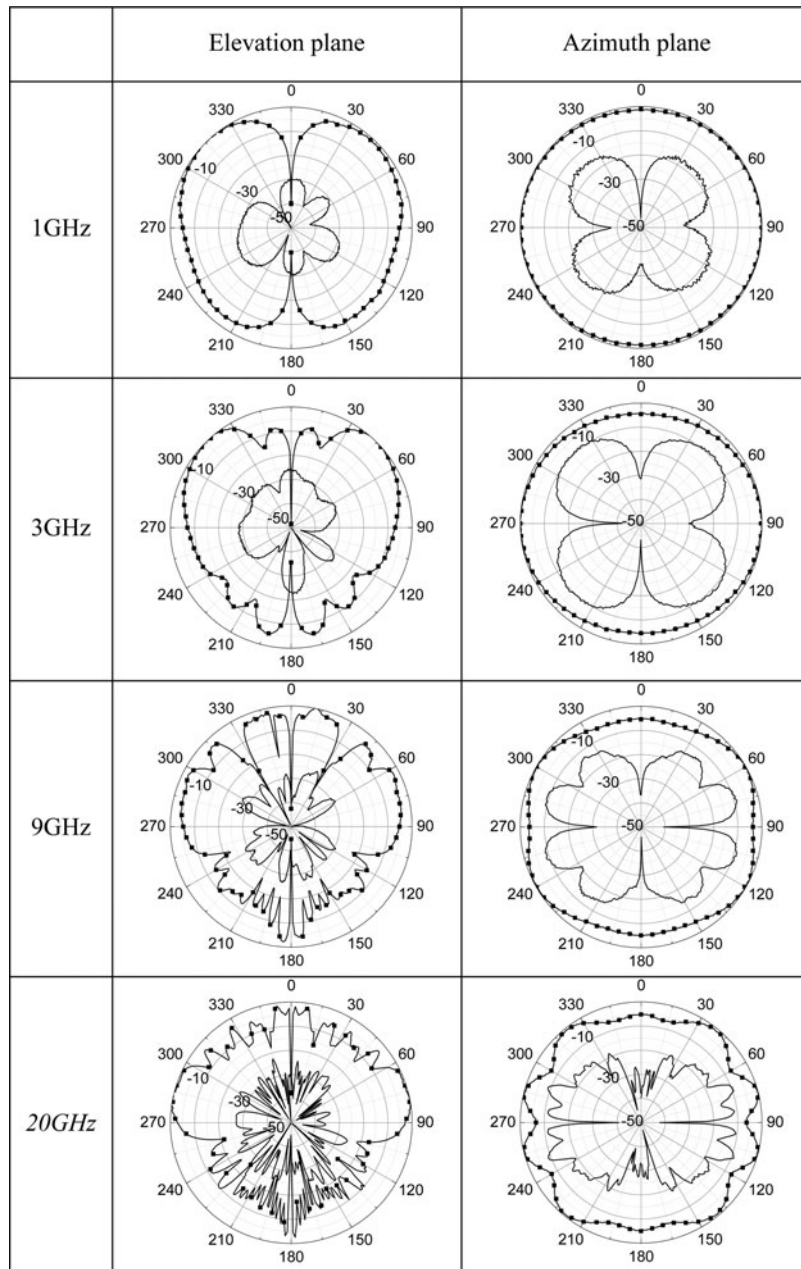


Fig. 10. Measured RPs (dB). —■— co-pol, — cross-pol.

time-domain properties are crucial for the antenna [13]. The group delay can clearly show the non-linearity of the phase response and indicate the degree of the distortion. We use two identical proposed antennas as transmitting terminal and receiving terminal to construct a UWB link, and the distance between them is 900 mm. As the antenna is not symmetrical, two cases are calculated. One is the two antennas are placed along x -axis basing on the coordinate system of Fig. 1(b); the other is along the y -axis. Figure 9 presents the two calculated group-delay curves of the UWB system. The results show, the maximum variations of two curves are 1.7 and 1.6 ns separately, which indicates good time-domain properties of the antenna for UWB applications [14].

The radiation properties of the antenna are also presented. We show the RPs of elevation plane (xoz -plane)

and azimuth plane (parallel xoy -plane cutting the peak gain) at 1, 3, 9, and 20 GHz. Figure 10 collects the results. The co-polarized RPs indicate that the proposed antenna has the like-monopole omnidirectional radiation in the whole band. As the frequency increases, the peak value in elevation plane changes from high elevation angle to low one, and the co-polarized ripple level (out-of-roundness) in azimuth plane also increases. Table 1 lists the ripple levels.

Table 1. Ripple levels and peak gains against frequency.

Frequency (GHz)	1	3	9	20
Ripple levels (dB)	1.1	4.2	5.0	6.6
Peak gain (dB)	3.8	6.3	5.0	8.7

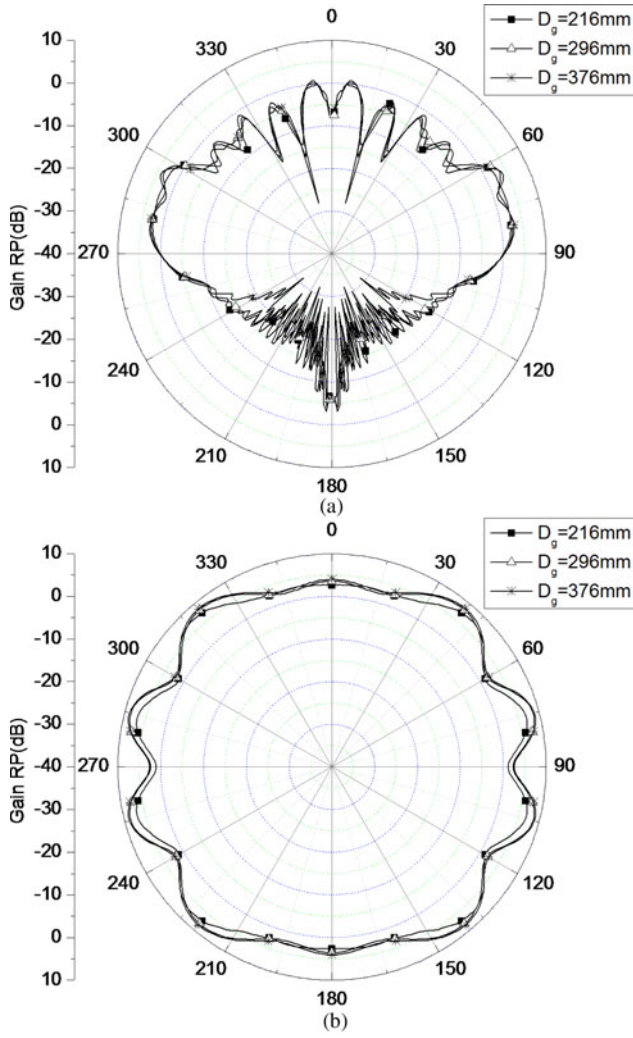


Fig. 11. RPs with different D_g at 20 GHz. (a) Elevation plane. (b) Azimuth plane.

The maximum ripple level is not more than 6.6 dB at 20 GHz, while this level is not more than 9.9 dB in [2]. It implies the proposed simple structure can bring an improved roundness. Meanwhile, the cross-polarized levels are also reduced, and the worst value is about -9 dB. In comparing reference, the cross-polarized levels are almost equal to the co-polarized ones in the high-frequency band. The peak gains are also given in Table 1. As the frequency rises, the peak gain increases from 3.8 to 8.7 dB.

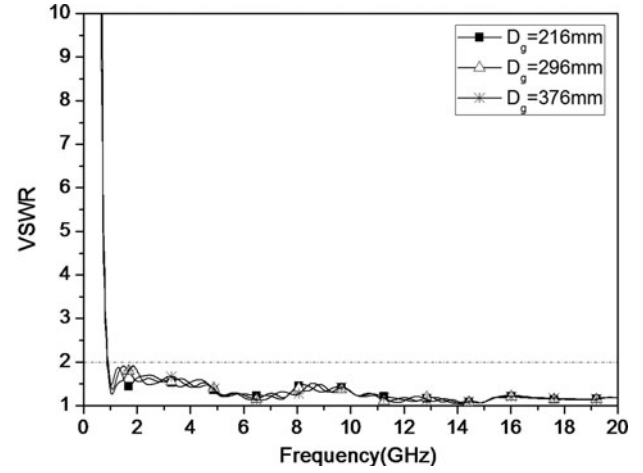


Fig. 12. VSWRs with different D_g .

As well known, the ground sizes of the omnidirectional antenna could affect the radiation properties, such as the elevation angle and the roundness of RPs. Here, we show the variation of the RPs at 20 GHz. Figure 11 shows the RPs of elevation plane and azimuth plane with three ground diameters, i.e. 216 mm ($0.651\lambda_c$), 296 mm ($0.893\lambda_c$), and 376 mm ($1.134\lambda_c$). We can obtain the ground diameter has a little effect on the radiation properties of the proposed antenna. The elevation angle almost has no change, and the out-of-roundness are 6.4, 6.6, and 6.6 dB separately. The corresponding VSWR curves are also given in Fig. 12. The SWB property is maintained well.

As the summary, Table 2 shows the comparison of the proposed antenna with several literature antennas with the impedance bandwidth of more than 1:4 [2, 10, 12]. From the given results, the proposed antenna indicates the comprehensive advantages in physical structures and performances.

V. CONCLUSION

A SWB and compact omnidirectional antenna is presented in the paper. The structure of the antenna is more practical and simpler than that of former SWB omnidirectional antenna, so the antenna is more suitable for the engineering. Meanwhile, the dimension of the antenna is also smaller than former SWB omnidirectional antenna. Through the simulation and the measurement, it is confirmed the antenna has the SWB

Table 2. Comparison of the proposed antenna with the literature antennas.

Antenna	Height	Radiation-body diameter	Ground diameter	Structure	Bandwidth	Peak gain (dB)	Roundness (dB)	Cross-pol. (dB)
Proposed antenna	$0.078\lambda_c$	$0.217\lambda_c$	$0.893\lambda_c$	Simple	$>1:22.1$	8.7	6.6	-9
Antenna in [2]	$0.087\lambda_c$	$0.240\lambda_c$	$0.920\lambda_c$	Complex	$>1:26$	9.5	9.9	0
Antenna* in [10]	$0.071\lambda_c$	$0.287\lambda_c$	$0.980\lambda_c$	Medium	$=1:6.51$	8.0	-	-10
Antenna in [12]	$0.086\lambda_c$	$0.228\lambda_c$	$0.923\lambda_c$	Medium	$>1:4$	-	-	-

Note: λ_c is the wavelength of the low cut-off frequency for $VSWR \leq 2$.

*The antenna is square shape, so its sizes are converted into the maximal diameters.

impedance property and the improved like-monopole RPs. Furthermore, the roundness of the antenna in azimuth plane is improved into not more than 6.6 dB, and the cross-polarized levels are reduced by 9 dB. Based on the results, the proposed antenna has more advantages when it is used in the multi-band and UWB mobile communication systems.

ACKNOWLEDGEMENTS

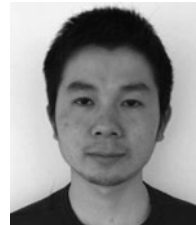
This work was supported in part by the Fundamental Research Funds for the Central Universities K5051202006, in part by the Xi'an Science and Technology Plan Project CXY1436②, and in part by the National Natural Science Funds of China (No. 61501362), P.R.C.

REFERENCES

- [1] Lau, K.L.; Li, P.; Luk, K.M.: A monopolar patch antenna with very wide impedance bandwidth. *IEEE Trans. Antennas Propag.*, **53** (2005), 655–661.
- [2] Lau, K.L.; Kong, K.C.; Luk, K.M.: Super-wideband monopolar patch antenna. *Electron. Lett.*, **44** (2008), 716–718.
- [3] Behdad, N.; Li, M.; Yusuf, Y.: A very low-profile, omnidirectional, ultra wideband antenna. *IEEE Antennas Wireless Propag. Lett.*, **12** (2013), 280–283.
- [4] Gong, B.; Li, J.L.; Zheng, Q.R.; Yin, Y.Z.; Ren, X.S.: A compact inductively loaded monopole antenna for future UWB applications. *Progr. Electromagn. Res.*, **139** (2013), 265–275.
- [5] Delaveaud, Ch.; Leveque, Ph.; Jecko, B.: New kind of microstrip antenna: the monopolar wire-patch antenna. *Electron. Lett.*, **30** (1994), 1–2.
- [6] Row, J.S.; Yeh, S.H.; Wong, J.L.: A wide-band monopolar plate-patch antenna. *IEEE Trans. Antennas Propag.*, **50** (2002), 1328–1330.
- [7] Lau, K.L.; Luk, K.M.: A wide-band monopolar wire-patch antenna for indoor base station application. *IEEE Antennas Wireless Propag. Lett.*, **4** (2005), 155–157.
- [8] Nakano, H.; Iwaoka, H.; Morishita, K.; Yamauchi, J.: A wideband low-profile antenna composed of a conducting body of revolution and a shorted parasitic ring. *IEEE Trans. Antennas Propag.*, **56** (2008), 1187–1192.
- [9] Zhang, Z.Y.; Fu, G.; Gong, S.X.; Lu, Q.Y.: Sleeve monopole antenna for DVB-H applications. *Electron. Lett.*, **46** (2010), 879–880.
- [10] Danial, W.A.; Randy, L.: A wideband, low profile, shorted top hat monocone antenna. *IEEE Trans. Antennas Propag.*, **60** (2012), 4485–4491.
- [11] Chen, X.; Fu, G.; Li, X.: Super wideband characteristics of monopolar patch antenna. *J. Eng.*, **1** (2013), 1–3.
- [12] Koohestani, M.; Zurcher, J.-F.; Moreira, A.A.; Skrivervik, A.K.: A novel, low-profile, vertical-polarized UWB antenna for WBAN. *IEEE Trans. Antennas Propag.*, **62** (2014), 1888–1894.
- [13] Gao, G.P.; Yang, M.K.; Niu, S.F.; Zhang, J.S.: Study of a novel U-shaped monopole UWB antenna by transfer function and time domain characteristics. *Microw. Opt. Technol. Lett.*, **54** (2012), 1532–1537.
- [14] Gao, G.P.; Hu, B.; Cong, X.D.; He, L.L.: Investigation of a novel dual band-notched UWB antenna by the equivalent circuit model and time domain characteristics. *Microw. Opt. Technol. Lett.*, **55** (2013), 2993–3000.



X. Chen received a bachelor degree in Electronic and Information Engineering from Xidian University in 2006 and received his Ph.D. degree in Electromagnetic Field and Microwave Technology in 2011. He now holds a research chair at Xidian University. His main research interests are theory and engineering of wideband antenna and array antenna.



L. Yang received a Bachelor degree in Electronic and Information Engineering from Xidian University in 2012 and received his Master degree in Electromagnetic Field and Microwave Technology in 2014. He is now working for his Ph.D. at Xidian University. His main research interests are theory and engineering of wideband antenna and circularly polarized antenna.



L. Wang received a Bachelor degree in Electronic and Information Engineering from Xidian University in 2012. He is now working for his Ph.D. at Xidian University. His main research interests are theory and engineering of array antenna.



G. Fu received a Bachelor degree in Electromagnetic Field and Microwave Technology from Xidian University in 1984 and received his Master degree in Electromagnetic Field and Microwave Technology in 1991. He became a full professor at Xidian University in 2001. His current research interests are theory and engineering of antenna.